Received: 16 March 2020 | Revised: 9 July 2020 | Accepted: 16 July 2020

DOI: 10.1096/fj.202000610RR

RESEARCH ARTICLE

THE FASEB JOURNAL

Brain delivery of biologics using a cross-species reactive transferrin receptor 1 VNAR shuttle

Dag Sehlin[1] | **Pawel Stocki**[2,3] | **Tobias Gustavsson**[1] | **Greta Hultqvist**[4] | **Frank S. Walsh**[2,3] | **J. Lynn Rutkowski**[2,3] | **Stina Syvänen**[1]

[1]Department of Public Health and Caring Sciences/Geriatrics, Uppsala University, Uppsala, Sweden

[2]Ossianix, Inc., Stevenage, UK

[3]Ossianix, Inc., Philadelphia, PA, USA

[4]Department of Pharmaceutical Biosciences, Uppsala University, Uppsala, Sweden

Correspondence
Dag Sehlin, Department of Public Health and Caring Sciences/Geriatrics, Uppsala University, 751 85 Uppsala, Sweden.
Email: dag.sehlin@pubcare.uu.se

Pawel Stocki, Ossianix, Inc., Gunnels Wood Rd, Stevenage, Herts, UK.
Email: pawel@ossianix.com

Funding information
Vetenskapsrådet (VR), Grant/Award Number: 2018-02715 and 2017-02413; Alzheimerfonden; Hjärnfonden (Swedish Brain Foundation); Torsten Söderbergs Stiftelse (Torsten Söderberg Foundation); Petrus och Augusta Hedlunds Stiftelse (Hedlund Foundation); Åke Wiberg Stiftelse (Åke Wiberg Foundation); Åhlénstiftelsen (Åhlén Foundation); Magnus Bergvalls Stiftelse (Magnus Bergvall Foundation); Gun och Bertil Stohnes Stiftelse (Stohnes Stiftelse); Stiftelsen för Gamla Tjänarinnor (Foundation for Old Servants); Stiftelsen Sigurd and Elsa Goljes Minne

Abstract

Transferrin receptor 1 (TfR1) mediated transcytosis is an attractive strategy to enhance brain uptake of protein drugs, but translation remains a challenge. Here, a single domain shark antibody VNAR fragment (TXB2) with similar affinity to murine and human TfR1 was used to shuttle protein cargo into the brain. TXB2 was fused to a human IgG1 Fc domain (hFc) or to the amyloid-β (Aβ) antibody bapineuzumab (Bapi). TXB2-hFc displayed 20-fold higher brain concentrations compared with a control VNAR-hFc at 18 hours post-injection in wt mice. At the same time point, brain concentrations of Bapi-TXB2 was threefold higher than Bapi. In transgenic mice overexpressing human Aβ, the brain-to-blood concentration ratio increased with time due to interaction with intracerebral Aβ deposits. The relatively stable threefold difference between Bapi-TXB2 and Bapi was observed for up to 6 days after injection. PET imaging and ex vivo autoradiography revealed more parenchymal distribution of Bapi-TXB2 compared with Bapi. In conclusion, the TXB2 VNAR shuttle markedly increased brain uptake of protein cargo and increased brain concentrations of the Aβ binding antibody Bapi.

KEYWORDS

Alzheimer's disease (AD), amyloid-β (Aβ), antibody, blood-brain barrier (BBB), positron emission tomography (PET), receptor mediated transcytosis

Abbreviations: Aβ, amyloid-β; AβPP, Aβ protein precursor; AD, Alzheimer's disease; BBB, blood-brain barrier; hFc, human fragment crystallizable region; PET, positron emission tomography; TfR1, transferrin receptor 1; tg-ArcSwe, AβPP transgenic mice with the Arctic and Swedish AβPP mutations; VNAR, variable domain of New Antigen Receptors; wt, wild-type.

1 | INTRODUCTION

Biologics are the fastest growing class of therapeutic agents. The majority of these drugs bind to peripheral targets, and there are also a number of drugs in clinical trials aimed for neurodegenerative diseases such as Alzheimer's disease (AD), Parkinson's disease (PD), and amyotrophic lateral sclerosis (ALS). Reducing amyloid-β (Aβ) pathology is one of the most explored therapeutic strategies in AD drug development although to date many clinical trials have failed to meet their clinical endpoints or have been terminated due to unacceptable side effects.[1]

One challenge when using antibodies or other biologics as therapeutics for the brain is their limited passage across the blood-brain barrier (BBB). The BBB limits the transport of molecules between blood and brain and the amount of peripherally administered antibody that reaches the brain is less than 0.1%[2] and it has even been questioned whether antibodies penetrate the brain parenchyma at all.[3]

There is a clear need for improved delivery systems for drugs to treat CNS disease. Various strategies have been described for targeted delivery across the BBB, for example, by using different receptors known to be present in the brain endothelium. One of the most studied approaches has been receptor mediated transcytosis by the transferrin receptor 1 (TfR1), either by direct fusion of a TfR1 binder to a protein cargo, for example, an antibody,[4] or by functionalizing cargo encapsulated nanocarriers with TfR1 binders or even Tf.[5-7] Utilizing the first approach, the therapeutic antibody is fused to an antibody or fragment of an antibody against the TfR1. This approach has been very efficient in preclinical studies and substantial increases in brain antibody concentrations have been reported by several groups.[8-10] However, this strategy has its challenges including faster plasma PK of IgG fusion proteins compared with unmodified IgG,[11] side effects such as reticulocyte lysis[12] and a lack of cross-species reactivity. Other potential shuttles, for example, antibodies binding to the endothelial cell surface protein CD98 and FC5 binding the transmembrane protein 50A (TMEM50A), have been described as cross-species reactive, but only a few studies have been reported on the in vivo efficacy to deliver large protein cargos across the BBB and the cross-species reactivity has not been investigated in detail.[13-15]

Recently a single domain VNAR (TXB2) shark antibody, which binds to TfR1 in a variety of species was described.[16] In the present study, we wished to investigate the ability of this VNAR to shuttle a biologic cargo into the brain and chose to study the well described therapeutic antibody *bapineuzumab* (Bapi) which targets Aβ.[17] Positron emission tomography (PET) and radioactivity measurements were used to image and quantify the uptake and intrabrain distribution in wild-type mice and transgenic mice over-expressing human Aβ.

2 | METHODS

2.1 | Analysis of TXB2 VNAR

TXB2 was expressed as a fusion protein with the human IgG1 Fc domain as reported previously.[16] A similar construct based on a VNAR clone, that binds to TfR1 with nanomolar affinity but does not penetrate brain, served as control (control VNAR-hFc).[16] VNAR-hFc formats were produced with VNARs at the N-terminal end of a human IgG1 Fc (Figure 1A), where a series of substitutions (E233P, L234V, L235A, ΔG236, A327G, A330S, P331S) were introduced to attenuate effector functions.[18]

For in vivo studies, in AβPP transgenic mice, TXB2 was fused to the Aβ binding humanized IgG1 antibody Bapi, attached to the N-terminal end of the antibody heavy chain via a 3xG4S linker (Figure 2A). Non-modified Bapi, used as control, as well as the Bapi-TXB2 construct contained a human IgG1 Fc domain with mutations in the lower hinge region (L234A, L235A, G237A) to reduce effector functions.

Proteins were produced using a transient transfection Exp293F expression system (Thermo Fisher) following the manufacturer's protocol. After 5 days, the medium was centrifuged and the filtered supernatant was used for protein purification on a HiTrap MabSelect SuRe column (GE Healthcare) followed by buffer exchange to PBS pH 7.4 using a HiPrep 26/10 Desalting column (GE Healthcare). Purity of the purified proteins was determined by analytical size exclusion chromatography (SEC) and SDS-PAGE.

2.2 | Animals

The AβPP transgenic mouse model tg-ArcSwe, harboring the Arctic (*AβPP E693G*) and Swedish (*AβPP KM670/671NL*) mutations, maintained on a C57BL/6 background were used in this study. Tg-ArcSwe mice show elevated levels of soluble Aβ protofibrils already at a very young age and abundant and rapidly developing plaque pathology, with high resemblance to human AD pathology, starting around 6 months of age.[19-21] Both male and female tg-ArcSwe mice were used (n = 20, 18-21 months old; n = 8, 12 months old). Wild-type mice (wt) were used in ex vivo studies of BBB uptake (n = 6, 18-21 months old; n = 13, 12 months old; n = 16, 3-4 months old) and as control animals in PET studies (n = 6, 18-21 months old). The animals were housed with free access to food and water in rooms with controlled temperature and humidity in an animal facility at Uppsala University. Animals that underwent PET-scanning were given water supplemented with 0.2% NaI one day prior to radioligand administration to reduce thyroidal uptake of iodine-124 (^{124}I), which can interfere with brain PET imaging. All procedures described

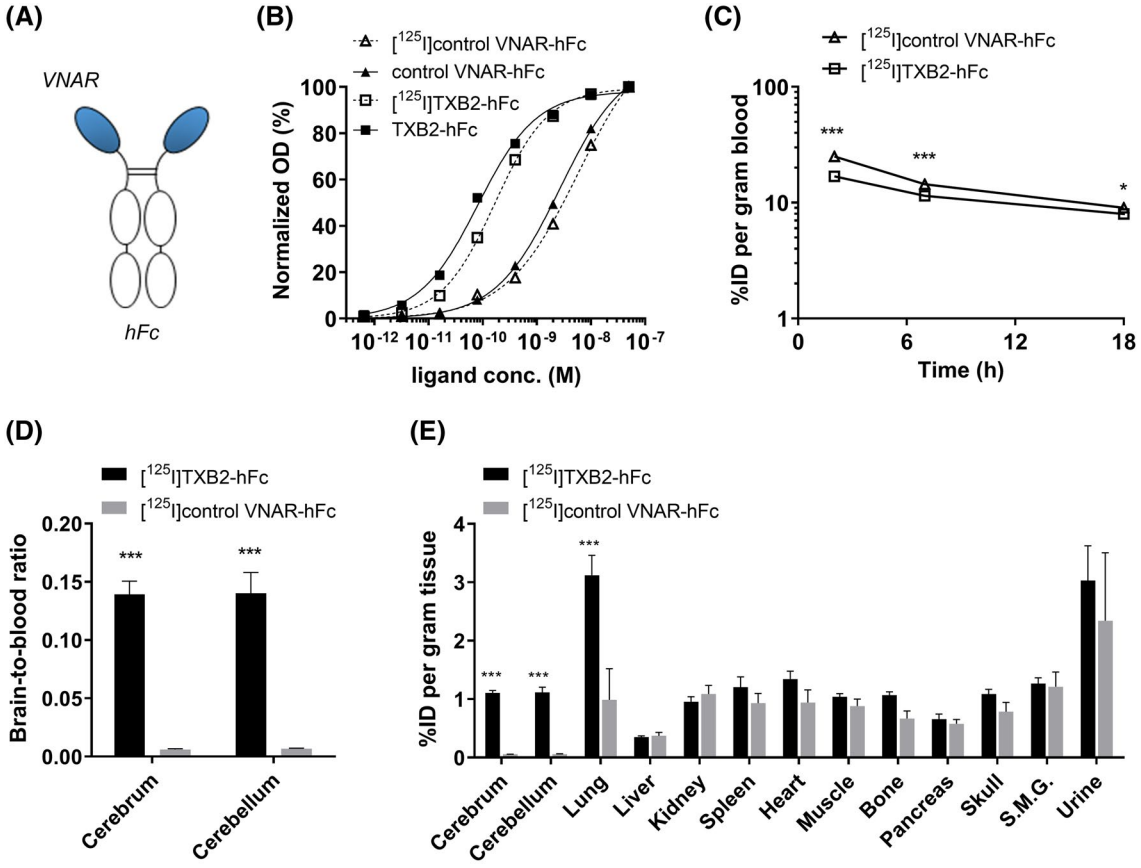

FIGURE 1 A, Schematic image of VNAR-hFc constructs, where the VNAR fragment was attached to the N-terminal end of a human Fc domain. B, TfR1 ELISA of ^{125}I-labeled and nonlabeled Fc-fusion proteins. Whereas ^{125}I-labeling had a minor effect on TXB2-hFc TfR1 affinity, almost no difference was seen between control VNAR-hFc and [^{125}I]control VNAR-hFc. C, Blood concentrations over time after intravenous administration of [^{125}I]TXB2-hFc and [^{125}I]control VNAR-hFc in wt mice (n = 4/group). D, Biodistribution to brain and major organs at 18 hours after intravenous administration of [^{125}I]TXB2-hFc and [^{125}I]control VNAR-hFc (n = 4/group). E, The brain-to-blood concentration ratio in cerebrum and cerebellum of [^{125}I]TXB2-hFc (n = 4) and [^{125}I]control VNAR-hFc (n = 4) at 18 hours after administration. SMG = submandibular glands

in this paper were approved by the Uppsala County Animal Ethics Board (#C17/14 and #5.18.18-13350/17), following the rules and regulations of the Swedish Animal Welfare Agency, and were in compliance with the European Communities Council Directive of 22 September 2010 (2010/63/EU).

2.3 | Radiochemistry

For ex vivo biodistribution studies, the antibody constructs were radioiodinated using the Chloramine T method as previously described.[22] Briefly, 36 μg of TXB2-hFc and control VNAR-hFc; 20 μg of Bapi or 24 μg of Bapi-TXB2 was mixed with 13.4 ± 2.0 MBq iodine-125 (^{125}I) stock solution (PerkinElmer Inc, Waltham, MA, USA) and 5 μg of Chloramine T (Sigma Aldrich) in PBS to a total volume of 110 μL and incubated for 90 seconds. The reaction was stopped with 10 μg of Na-metabisulfite (Sigma-Aldrich), followed by dilution up to 500 μL in PBS, then immediately, purified from non-reacted ^{125}I with a disposable NAP-5 size exclusion chromatography column (GE Healthcare, Uppsala, Sweden). ^{125}I labeled protein was eluted from the column with 1 mL sterile filtered PBS. For PET studies, Bapi and Bapi-TXB2 were radiolabeled with ^{124}I using a similar protocol. In short, 138 ± 3.8 MBq ^{124}I stock solution (PerkinElmer Inc) was pre-incubated with 14 μL 50 μM NaI for 20 minutes, followed by addition of 80 μg Bapi or Bapi-TXB2, 40 μg Chloramine T, and PBS to a final volume of 420 μL. After 120 seconds, the reaction was stopped with 80 μg Na-metabisulfite and the preparation was purified with a NAP-5 size exclusion chromatography column as above. Radiolabeling yield was calculated as eluted activity (attached to the protein) divided by total added activity. Labeling was performed less than 2 hours before injections. Antibody concentration after radiolabeling was determined with anti-IgG sandwich ELISA as described below. Radiochemical purity and stability of radiolabeled antibodies was assessed by incubation in mouse plasma for 6 days, followed by analysis with

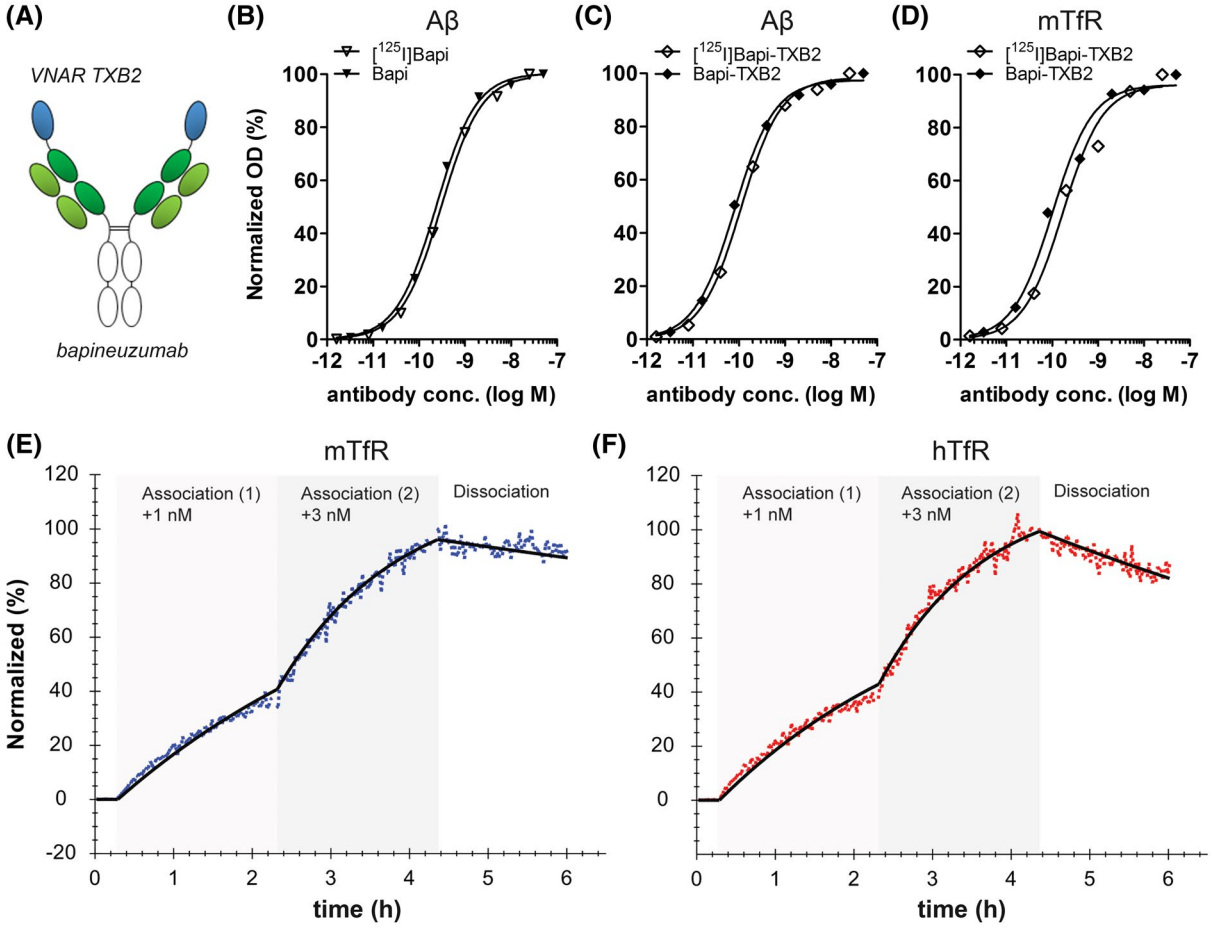

FIGURE 2 A, Schematic image of the Bapi-TXB2 construct, where the TXB2 VNAR fragment (in blue) was attached to the N-terminus of each of the Bapi heavy chains (in dark green). Aβ ELISA of Bapi (B) and Bapi-TXB2 (C) before and after radiolabeling. (D) Bapi-TXB2 binding to murine TfR1 assessed with ELISA before and after radiolabeling. [^{125}I]Bapi-TXB2 binding to murine (E) and human (F) TfR1 was studied in detail with Ligand Tracer, showing the ligand's association and dissociation to TfR1

radio-SDS-PAGE and radio-instant thin layer chromatography (ITLC), as previously described.[23]

2.4 | Biochemical analysis of TfR1 and Aβ binding

The extracellular domain of mTfR1 (Cys 89-Phe 763) and hTfR1 (Cys 89-Phe 760), both fused to a His-tag at the N-terminus, was produced by transient transfection of Expi293 cells. Proteins were purified from cell medium with nickel affinity chromatography and analyzed for purity with SDS-PAGE. The proteins were aliquoted in PBS and kept in −20°C until further use.

ELISA was used to assess mTfR1 and Aβ binding of ^{125}I and ^{124}I labeled proteins as well as antibody concentration after radiolabeling. A 96-well half-area plate (Corning) was coated over night with 25 ng/well of recombinant TfR1 protein, 22.5 ng/well of synthetic Aβ42 (American Peptide, Sunnyvale, CA, USA) or 50 ng/well of anti-human IgG (Mabtech Ab, Nacka Strand, Sweden), then, blocked with 1% of BSA in PBS. Unmodified and radiolabeled proteins were serially diluted from 50 nM and incubated for 2 hours at room temperature on a shaker, followed by a 2 hours incubation with HRP-conjugated polyclonal goat anti-human-IgG-F(ab′)$_2$ antibody (Jackson ImmunoResearch Laboratories, West Grove, PA, USA), diluted 1:2000 or goat anti-human IgG-Fc antibody (ThermoFisher, cat.# A18811), diluted 1:1000. Signals were developed with K Blue Aqueous TMB substrate (Neogen Corp., Lexington, KY, USA) and read with a spectrophotometer at 450 nm. Antibody dilutions were made in ELISA incubation buffer (PBS, 0.1% BSA, 0.05% Tween-20).

2.5 | Ligand Tracer

A simultaneous comparison of [^{125}I]Bapi-TXB2 binding to mTfR1 and hTfR1 was performed with a Ligand Tracer Grey instrument (Ridgeview Instruments AB, Uppsala, Sweden) as previously described.[24] In brief, mTfR1 and hTfR1 protein (10 μg/mL in PBS; 300 μL) was coated over night at

4°C on two local spots of a circular Petri dish, followed by blocking with 1% of BSA in PBS. The dish was placed in the Ligand Tracer instrument to record a baseline for 15 minutes. Radiolabeled [^{125}I]Bapi-TXB2 was then added at a concentration of 1 nM (2 mL in PBS 0.1% BSA) to measure its binding to the two TfR1 coated spots in comparison with a noncoated spot on the same dish. [^{125}I]Bapi-TXB2 association to TfR1 was recorded in real-time for 2.5 hours and the procedure was repeated with a 2.5 hours association of 3 nM [^{125}I]Bapi-TXB2, followed by a wash and dissociation overnight in 2 mL of PBS 0.1% BSA. Association and dissociation rate constants, k_a and k_d, as well as the resulting affinity constant K_D, were calculated with Trace Drawer 1.8.1 software (Ridgeview Instruments AB).

2.6 | Ex vivo and biodistribution studies

The radiolabeled proteins [^{125}I]TXB2-hFc and [^{125}I]control VNAR-hFc were injected into the tail vein of wt mice under mild isoflurane (Baxter Medical AB, Kista, Sweden) anesthesia. Injections were given at 5 μL/g mouse, resulting in a dose of 2.3 ± 0.1 nmol/kg body weight. Blood samples were obtained with 8 μL capillaries at 2 and 7 hours post-injection and a terminal blood sample was taken from the heart at 18 hours before animals were euthanized by intracardiac perfusion with 50 mL saline over 2 minutes. The 18 hours time point was based on previously determined T_{max} for TXB2.[16] To assess biodistribution of the radiolabeled proteins in brain as well as peripheral organs, lung, liver, kidney, spleen, heart, muscle, femoral bone, pancreas, skull, submandibluar glands, cerebrum, and cerebellum were isolated. Two animals administered with [^{125}I]TXB2-hFc were euthanized already at 2 hours after administration and brain was isolated after intracardiac perfusion in order to study the brain distribution at an early time point. Radioactivity was measured in blood and organs with a γ-counter (2480 Wizard, PerkinElmer, Waltham, USA) and concentrations were expressed as % of injected dose per gram tissue (% ID/g).

To investigate the ability of TXB2 to carry a relevant therapeutic antibody across the BBB, [^{125}I]Bapi and [^{125}I]Bapi-TXB2 (0.54 ± 0.06 nmol/kg body weight) were administered to wt and 12 or 18 month old tg-ArcSwe mice. Brain and peripheral organs were isolated after intracardiac perfusion from wt mice at 2, 18, 72, or 144 hours after administration according to the same procedure as above. In addition, [^{125}I]TXB2-hFc was injected in 18 month old tg-ArcSwe animals and perfused at 144 hours. Blood samples (8 μL) were obtained at 1, 3, 24, 48, 72, 96, and 144 hours. Time points were chosen to adhere with PET experiments (see next section). Radioactivity was measured and expressed as %ID/g.

2.7 | PET studies

[^{124}I]Bapi (specific activity 241 MBq/nmol) or [^{124}I]Bapi-TXB2 (specific activity 257 MBq/nmol) was administered at a dose of 1.7 ± 0.3 nmol/kg body weight to 18-21 months old tg-ArcSwe (n = 4 per group) and wt mice (n = 3 per group). Blood samples (8 μL) were obtained at 1, 3, 24, 48, 72, 120, and 144 hours. All mice were scanned at 6 days post-administration. This time point was chosen to enable visualization of Aβ with adequate contrast, that is, a high specific-to-unspecific signal. At earlier time points, unbound radiolabeled antibody in the brain as well as radiolabeled antibody in the blood volume of the brain may mask the specific signal arising from antibody bound to Aβ.

During PET-scanning mice were anaesthetized with isoflurane (2.5% in medical air) and placed in a prone position in a Triumph Trimodality System PET/CT scanner (TriFoil Imaging, Inc, Northridge, CA, USA). PET data was collected in list mode for 60 minutes followed by a CT examination for 3 minutes (Field of View (FOV) = 8.0 cm). PET data was reconstructed using the ordered subsets expectation-maximization (OSEM) 3D algorithm (20 iterations) and CT raw files were reconstructed using Filtered Back Projection (FBP). All processing of PET and CT images was performed using imaging software Amide 1.0.4.[25] A T2 weighted, MRI-based mouse brain atlas[26] containing outlined regions of interests for hippocampus, striatum, thalamus, cortex, and cerebellum was manually aligned with the CT scan, which was then aligned with the PET, thus, transferring the regions of interest to the PET image. PET images displaying %ID/g or the brain-to-blood concentration ratio were constructed.

Mice were euthanized directly after PET-scanning followed by isolation of blood, brain, and major organs. The brain was divided into the pieces; the right hemisphere, cerebrum of the left hemisphere, and cerebellum of the left hemisphere. Radioactivity in these samples was measured in a γ-counter and expressed as %ID/g.

2.8 | Ex vivo autoradiography, immunostaining, and nuclear track emulsion

To visualize distribution of Bapi and Bapi-TXB2 in the brain with ex vivo autoradiography, 20 μm thick sagittal cryosections were prepared from the right hemisphere isolated from mice injected with [^{125}I]Bapi or [^{125}I]Bapi-TXB2. The sections were placed in an X-ray cassette along with ^{125}I standards of known radioactivity. Positron-sensitive phosphor screens (MS, MultiSensitive, PerkinElmer, Downers grove, IL, USA) were placed onto the samples for five days of exposure and then scanned at a resolution of 600 dots per inch in a Cyclone Plus Imager

TABLE 1 Binding characteristics of Bapi and Bapi-TXB2 assessed with ELISA (a) and Ligand Tracer (b)

a. ELISA		K_D (M) *Aβ*		K_D (M) mTfR1
Bapi		$2.3 \cdot 10^{-10}$		n.a.
[^{125}I]-Bapi		$3.0 \cdot 10^{-10}$		n.a.
Bapi-TXB2		$8.0 \cdot 10^{-11}$		$1.0 \cdot 10^{-10}$
[^{125}I]Bapi-TXB2		$1.1 \cdot 10^{-10}$		$1.7 \cdot 10^{-10}$
b. Ligand Tracer	K_D (M)	k_a (1/(M•s))	k_d (1/s)	
[^{125}I]Bapi-TXB2 mTfR1	$2.5 \cdot 10^{-10} \pm 7.2 \cdot 10^{-11}$	$5.7 \cdot 10^{4} \pm 1.3 \cdot 10^{4}$	$1.4 \cdot 10^{-5} \pm 1.3 \cdot 10^{-6}$	
[^{125}I]Bapi-TXB2 hTfR1	$6.5 \cdot 10^{-10} \pm 9.5 \cdot 10^{-11}$	$7.1 \cdot 10^{4} \pm 1.4 \cdot 10^{4}$	$4.6 \cdot 10^{-5} \pm 1.4 \cdot 10^{-5}$	

Note: Ligand Tracer data is presented as mean ± SD, n = 3.

system (Perkin Elmer). The resulting digital images were converted to a false color scale (Royal) with ImageJ and normalized to the standards.

For a more detailed assessment of intrabrain antibody distribution, cryosections were fixated 10 minutes in ice cold methanol, rinsed with PBS and blocked with 5% of normal goat serum. Following a 5 minutes incubation with PBS 0.1% Tween 20, sections were incubated overnight with a mix of rat-anti mouse CD31 (BD) and rabbit-anti Aβ42 (custom produced, Agrisera, Umeå, Sweden), then, detected with fluorescently conjugated goat anti-rat/rabbit antibodies. After washing in TBS, sections were immediately submerged in 50% Ilford K5 emulsion, air dried for 2 hours, and then, stored in darkness for 2 weeks, followed by development as recommended by the manufacturer. Stainings were visualized with a Zeiss Observer Z.1 microscope using ZEN 2.6 software (Carl Zeiss Microimaging GmbH, Jena, Germany) and processed in Adobe photoshop 2020, where inverted bright-field images of track emulsion staining were combined with the fluorescent signals from anti-CD31 and Aβ stainings.

2.9 | Statistical analyses

Results are presented as mean ± standard deviation. Data were analyzed with one- or two-way analysis of variance (ANOVA) followed by Bonferroni's or Dunnett's post hoc test or with student's *t* test. Statistical analyses as well as plasma curve fit (one phase decay) were calculated with GraphPad Prism 6.07 (GraphPad Software, Inc, La Jolla, CA, USA).

3 | RESULTS

3.1 | Properties of constructs TXB2-hFc and control VNAR-hFc

TXB2-hFc and control VNAR-hFc (Figure 1A) were radiolabeled with a yield of 59.9% and 76.6% and a specific activity of 23.9 and 30.5 MBq/nmol, respectively. TfR1 ELISA analysis revealed that iodination had a minor impact on mTfR1 affinity of both constructs with the following estimated K_D values: TXB2-hFc—$8.1 \cdot 10^{-11}$ M; [^{125}I]TXB2-hFc—$1.7 \cdot 10^{-10}$ M; control VNAR-hFc—$2.7 \cdot 10^{-9}$ M; [^{125}I]control VNAR-hFc—$5.7 \cdot 10^{-9}$ M (Figure 1B).

Mice were intravenously (iv) administered [^{125}I]TXB2-hFc or [^{125}I]control VNAR-hFc. Blood samples obtained at 2, 7, and 18 hours post-injection showed that [^{125}I]TXB2-hFc initially disappeared somewhat faster than [^{125}I]control VNAR-hFc from blood resulting in 50% higher blood concentration of [^{125}I]control VNAR-hFc at 2 hours ($P < .001$). Concentrations of the two compounds in blood at 18 hours were more similar compared with earlier time points, although still significantly different ($P = .023$) (Figure 1C). The half-life in blood, measured from 2 to 18 hours was similar; 4.1 hours (95% CI 3.0-6.5 hours) and 3.4 hours (95% CI 2.5-5.1 hours) for [^{125}I]TXB2-hFc and [^{125}I]control VNAR-hFc, respectively.

The brain concentration and the brain-to-blood concentration ratio at 18 hours post-administration of [^{125}I]TXB2-hFc was about 20-fold higher than what was observed for [^{125}I]control VNAR-hFc (Figure 1D,E). The brain concentration of [^{125}I]TXB2-hFc at 18 hours was around 1% of the injected dose per gram brain tissue (Figure 1E) which was somewhat increased to what was found in two brains that were isolated at 2 hours post-administration (0.73 respective 0.76 %ID/g). There were no differences at 18 hours in concentrations in any other organs between the two ligands except in the lung that contained more [^{125}I]TXB2-hFc than [^{125}I]control VNAR-hFc, potentially as a consequence of high TfR1 expression in lung tissue in combination with the higher TfR1 affinity of TXB2 (Figure 1E).

3.2 | Assessment of constructs Bapi and Bapi-TXB2

Bapi and Bapi-TXB2 (Figure 2A) were radiolabeled with ^{125}I with a yield of 83.8% and 79.4% and a specific activity of 99.2 and 94.5 MBq/nmol, respectively. Antibody

concentration was unaffected by the radiolabeling procedure and the radiolabeled antibodies were stable in mouse plasma in vitro at 37°C over a period of 6 days, without signs of fragmentation and with retained high radiochemical purity >99% (Figure S1A-F). ELISA analyses showed that radiolabeling had only limited effect on Aβ and TfR1 binding of the two constructs (Figure 2B-D and Table 1a). A detailed comparison of the in vitro binding of [^{125}I]Bapi-TXB2 to murine and human TfR1 was performed with Ligand Tracer, which allows real time measurement of a ligand's association and dissociation. [^{125}I]Bapi-TXB2 was found to bind with high affinity to both murine and human TfR1, with slightly but significantly (P = .0046) different K_D values of 0.25 and 0.65 nM, respectively, mainly driven by a significantly (P = .011) faster dissociation rate for hTfR1 compared with mTfR1 (Figure 2E-F and Table 1b).

Animal studies revealed, that at 2 hours after administration, the brain concentrations and the brain-to-blood concentration ratio was threefold higher in wt mice administered with [^{125}I]Bapi-TXB2 than in wt mice administered with [^{125}I]Bapi. A threefold difference was also observed after 18 hours, while this difference decreased at later time points (Figure 3A,B). The maximum brain concentrations were observed from 2 hours up to 18 hours. Thereafter, brain concentrations decreased with decreasing blood concentrations (Figure 3A). Although blood concentrations initially appeared similar for the two ligands, [^{125}I]Bapi-TXB2 was eliminated faster than [^{125}I]Bapi from blood and concentrations became significantly ($P < .05$) different at 48 hours after administration (Figure 3A). The half-life in blood, calculated from 2 hours to 144 hours was 21 hours (95% CI 16-30 hours) and 22 hours (95% CI 18-29 hours) for [^{125}I]Bapi-TXB2 and [^{125}I]Bapi, respectively. However, if half-life in blood was calculated during the true elimination phase, that is, from 24 hours and onward, the half-life was 30 and 55 hours for [^{125}I]Bapi-TXB2 and [^{125}I]Bapi, respectively. In wt mice, the

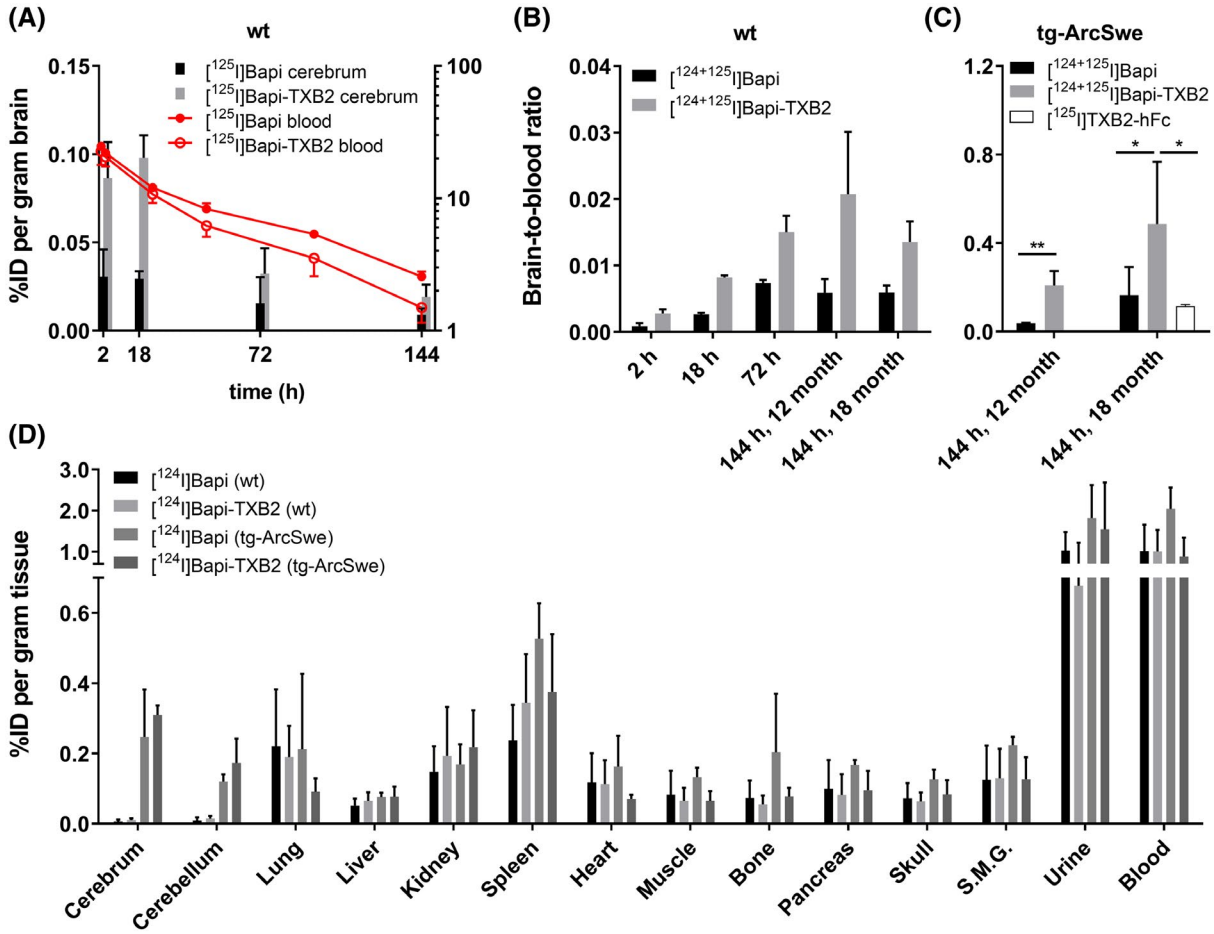

FIGURE 3 Brain and blood concentrations, expressed as percent of injected dose (%ID) per gram of brain tissue or blood (A), and brain-to-blood concentration ratio (B) of Bapi and Bapi-TXB2, radiolabeled with ^{124}I or ^{125}I in wt mice, at 2-144 hours after intravenous administration. C, Brain-to-blood concentration ratio of radiolabeled Bapi, Bapi-TXB2, or TXB2-hFc, 144 hours after injection in tg-ArcSwe mice. D, Biodistribution to brain and major organs at 144 hours after administration of [^{124}I]Bapi and [^{124}I]Bapi-TXB2 in PET scanned 18-month-old animals. SMG = submandibular glands. Number of mice: wt, n = 43 (A and B); 12 month tg-ArcSwe, n = 8 (C); 18 month tg-ArcSwe, n = 17 (C), n = 7 (D); 18 month wt, n = 6 (D). Statistical difference between antibody brain-to-blood ratios in (C) was tested separately in the two age groups with student's t test or one-way ANOVA (*$P < .05$, **$P < .01$)

brain-to-blood concentration ratio of Bapi increased with time up to 72 hours before becoming stable, while the ratio kept increasing also until 144 hours for Bapi-TXB2 (Figure 3B). The time-dependent increase in the brain-to-blood ratio was most likely a consequence of slower elimination from brain compared with the elimination from blood. Both Bapi and Bapi-TXB2 were retained, specifically bound to Aβ, in the brains of tg-ArcSwe mice, and thus, displayed a higher brain-to-blood ratio in tg-ArcSwe mice than in wt mice. Bapi-TXB2 displayed a significantly higher ratio than Bapi in both the 12 and 18 month tg-ArcSwe groups ($P = .0019$ and $P = .026$, respectively) (Figure 3C). Furthermore, in accordance with a more advanced Aβ pathology in aged mice, the ratio was higher in 18 months compared to 12 months old tg-ArcSwe animals (Figure 3B,C, Table 2). TXB2-hFc, which does not have an Aβ binding domain, showed a significantly lower brain-to-blood ratio than Bapi-TXB2 in tg-ArcSwe mice 144 hours after injection (Figure 3C). This result suggests that the increased brain retention of Bapi-TXB2 is due to a combination of increased brain penetration and binding to intrabrain deposits of Aβ, but not to a general leakiness of the tg-ArcSwe BBB. Further, in vivo stability assessment of the radiolabeled antibodies showed negligible degradation in both plasma and brain 144 hours after injection (Figure S1G,H).

After ex vivo studies, Bapi and Bapi-TXB2 were radiolabeled with the PET compatible radionuclide ^{124}I and administered to old tg-ArcSwe and age-matched wt mice. Blood concentrations were not significantly different in the different groups although there was a trend showing a somewhat slower clearance of [^{124}I]Bapi compared with [^{124}I]Bapi-TXB2 especially in tg-ArcSwe mice (Figure 3D). PET images obtained at 6 days confirmed this observation as radioactivity in tissue surrounding the head region, which correlates to blood concentrations, appeared higher in the tg-ArcSwe [^{124}I]Bapi group than in the other groups (Figure 4A). The concentration of the two ligands in major organs, except the brain, was similar in all groups (Figure 3D). In the brain, both [^{124}I]Bapi and [^{124}I]Bapi-TXB2 concentrations were higher in tg-ArcSwe compared with wt mice. The same was observed for the brain-to-blood concentrations ratio (Figure 3B,C, Table 2).

To compensate for the higher blood concentrations in the Bapi mice as well as for differences in elimination of the ligands within groups, PET images were scaled to the blood concentration of [^{124}I]Bapi and [^{124}I]Bapi-TXB2 and displayed as brain-to-blood concentration ratios (Figure 4B). Using this normalization, tg-ArcSwe mice administered with [^{124}I]Bapi-TXB2 showed the highest signal in the brain compared with the other three groups.

We have previously reported that a radiolabeled murine variant of Bapi, [^{125}I]3D6, accumulates as hot spots in vessels of old tg-ArcSwe mice, bound to vascular amyloid deposits.[27] This vascular accumulation could contribute to the relatively high brain retention of [^{124}I]Bapi in 18 month old tg-ArcSwe mice observed with PET. It could also explain why the difference in brain-to-blood ratio between Bapi-TXB2 and Bapi was higher in 12 month (5.6-fold difference) compared to 18 month (3.0-fold difference) tg-ArcSwe mice (Table 2). We, therefore, performed ex vivo autoradiography on brain sections from [^{125}I]Bapi and [^{125}I]Bapi-TXB2 injected 12-month-old tg-ArcSwe mice, which may have less vascular amyloid pathology due to their younger age, and compared to 18 month old mice. Both [^{125}I]Bapi and [^{125}I]Bapi-TXB2 appeared as hot spots in the brain tissue, although to a lesser extent in 12 months old mice. Notably, the amount of spots seemed less abundant in [^{125}I]Bapi-TXB2 injected brains compared to [^{125}I]Bapi injected brains of mice at both ages. The [^{125}I]Bapi-TXB2 brains also appeared to have a clear pattern of evenly distributed signal in regions where Aβ pathology is abundant (Figure 5A). To study antibody distribution in detail, nuclear track emulsion autoradiography was performed in combination with immunostaining of Aβ and the vascular marker CD31 in 18 month old tg-ArSwe mice at 144 hours after injection of [^{125}I]Bapi and [^{125}I]Bapi-TXB2. These analyses revealed that [^{125}I]Bapi could not be

TABLE 2 Bapi and Bapi-TXB2 brain-to-blood concentration ratios at 144 hours after injection

Blood-to-brain concentration ratio	wt	Tg-ArcSwe	Difference tg-ArcSwe vs wt
Bapi			
12 months	0.006 ± 0.002 (n = 6)	0.037 ± 0.003 (n = 4)	6.03-fold
18 months	0.006 ± 0.001(n = 6)	0.164 ± 0.128 (n = 6)	27.7-fold
Bapi-TXB2			
12 months	0.021 ± 0.009(n = 7)	0.209 ± 0.065 (n = 4)	10.1-fold
18 months	0.014 ± 0.003 (n = 6)	0.486 ± 0.281 (n = 7)	35.9-fold
Difference Bapi-TXB2 vs *Bapi*			
12 months	3.5-fold	5.6-fold	
18 month	2.3-fold	3.0-fold	

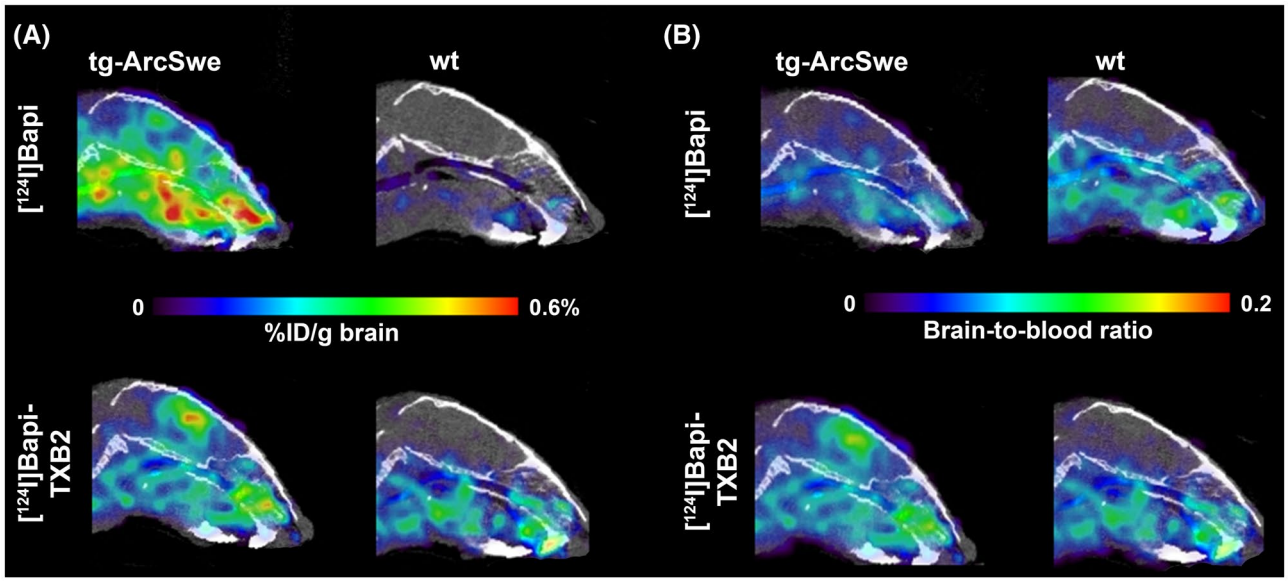

FIGURE 4 A, Representative PET images scaled to percent of injected ligand per gram brain show higher concentrations of both [^{124}I]Bapi and [^{124}I]Bapi-TXB2 in tg-ArcSwe brain compared with wt. B, Representative PET images scaled to the concentration in blood to compensate for differences in systemic elimination show the highest signal in with [^{124}I]Bapi-TXB2 in tg-ArcSwe mouse brain. The same mice are displayed in a and b, n = 4 in tg-ArcSwe groups and n = 3 in wt groups

found in the brain parenchyma (Figure 5B), while [^{125}I]Bapi-TXB2 was found in the vicinity of parenchymal Aβ plaques (Figure 5C). Both antibodies appeared as hot spots, in and around vessels with Aβ deposits (Figure 5D).

4 | DISCUSSION

Receptor mediated transport across the BBB is increasingly viewed as an attractive approach to considerably enhance brain concentrations of therapeutic antibodies and other biologics. However, there have been perceived limitations of this approach at the level of pharmacokinetics,[9,11] dosing,[28] side effects,[12] and translatability to larger species.[13,14]

The present study assesses the utility of a single domain VNAR antibody (TXB2) to TfR1 to deliver a radiolabeled Aβ antibody into the brain of AβPP transgenic mice. The TXB2-VNAR showed high affinity binding, with similar K_D values, to both mTfR1 and hTfR1 although with somewhat slower dissociation from mTfR1 compared with hTfR1. It is however difficult to conclude if this difference will have an impact on BBB transcytosis in vivo. As indicated by several studies, moderate TfR1 affinity, as well as monovalent TfR1 binding may be advantageous for efficient transport across the BBB of particular antibodies, for example, 8D3.[8,10] However, the exact mechanism for TfR1 mediated transcytosis is not entirely understood and additional features may also be important for a good brain shuttle.

Ex vivo experiments with TXB2 fused to a human IgG Fc domain clearly showed the potential of the TXB2-VNAR to deliver a protein cargo into the brain. At 18 hours post-injection in wt mice, TXB2-hFc displayed approximately 20-fold higher brain concentrations compared to a control bispecific protein, control VNAR-hFc, which has been developed as a negative control and found to be unable to mediate transcytosis.[16] When TXB2 was fused to the therapeutic antibody *Bapi* (Bapi-TXB2), brain concentrations in wt mice increased threefold compared with unmodified Bapi antibody 18 hours post-injection. These results show that TXB2 is more efficient in facilitating brain distribution of the Fc domain compared to the full-length IgG. Whether this difference is dependent of the fusion protein formats or the size of the cargo was not studied here, but other TfR1 binders, such as the well-studied mTfR1 antibody 8D3, do not seem to be much affected by cargo size; we have previously shown that 8D3 can efficiently shuttle both a full size IgG[9] and a 28 kDa single chain antibody fragment (scFv).[29] Additional factors, such as orientation of the VNAR on IgG, valency of TfR1 binding as well as IgG glycosylation may also play an important role.

The pharmacokinetic studies showed that with time, brain concentrations of both ligands decreased as the ligand was eliminated both from brain and blood. The difference between Bapi and Bapi-TXB2 in brain concentration also decreased with time due to a somewhat faster clearance of Bapi-TXB2 compared with Bapi, but the brain-to-blood ratio in wt mice remained threefold higher for Bapi-TXB2 up to 6 days after injection.

PET imaging was performed to investigate the spatial distribution of the two ligands in the brain. The optimal time point for PET scanning depends to a large degree on the brain-to-blood concentration ratio, rather than the brain

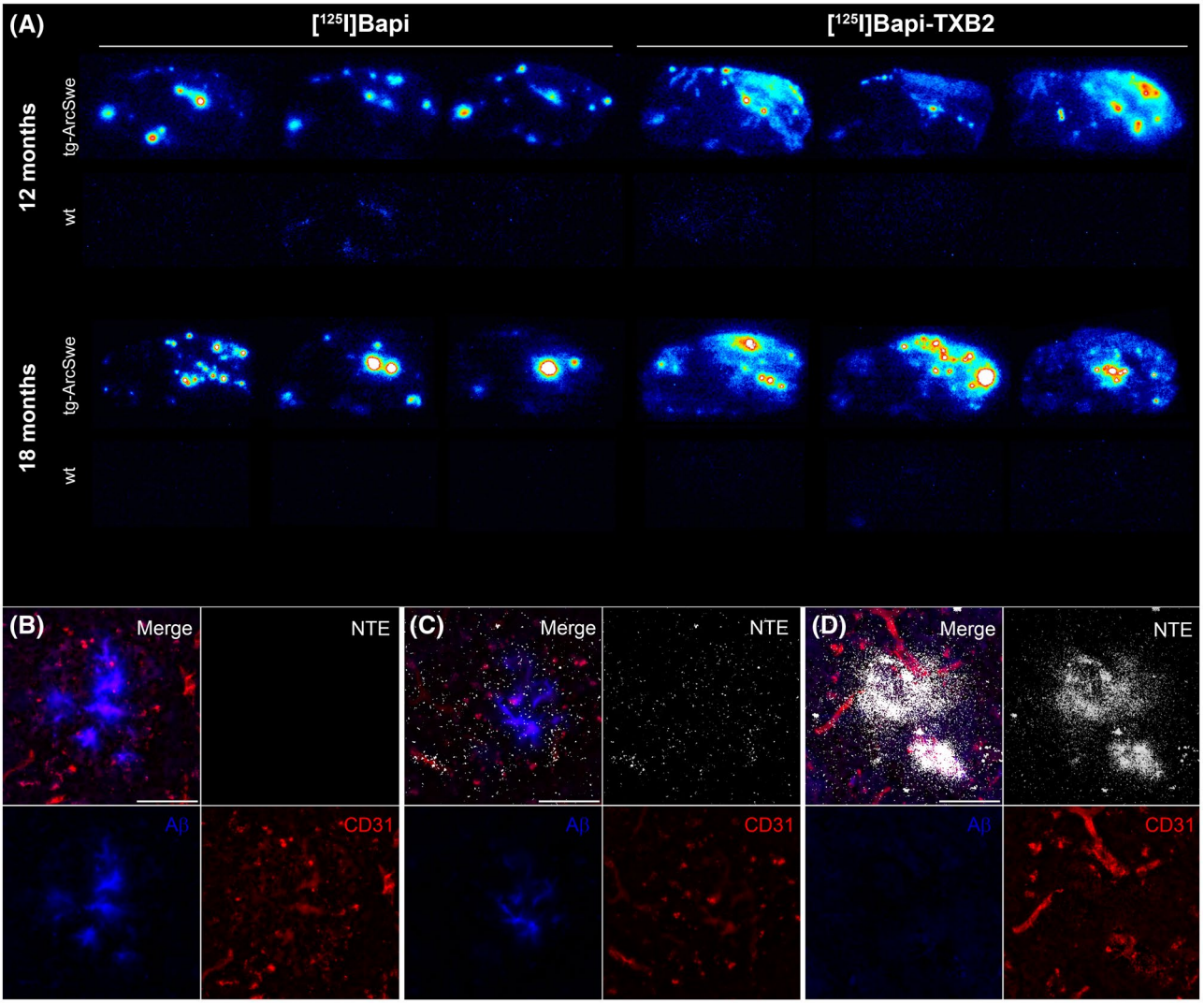

FIGURE 5 A, Autoradiography images of brain sections from [^{125}I]Bapi and [^{125}I]Bapi-TXB2 injected 12- and 18-month-old tg-ArcSwe and wt mice (n = 3 per group). In tg-ArcSwe mice, [^{125}I]Bapi was retained in hot spots, likely bound to vascular Aβ deposits. This phenomenon was observed in both age groups, but was more prominent in older mice. [^{125}I]Bapi-TXB2 not only had a more widespread retention pattern in cortical areas, where parenchymal Aβ pathology is found, but was also retained in hot spots, especially in old mice. In wt brains, no clear signal was observed. High intensity colors represent high radioactivity signal. Radiolabeled antibodies were visualized in greater detail with nuclear track emulsion autoradiography (white dots) combined with immunostaining for the vascular marker CD31 (red) and Aβ (blue). Parenchymal Aβ plaques in [^{125}I]Bapi injected mice were not associated with antibody signal (B), whereas [^{125}I]Bapi-TXB2 was found in the parenchyma around Aβ deposits (C). All animals showed some degree of hot spots, representing particularly high local accumulation of antibody around vascular Aβ deposits (D). Merged image as well as a separate image for each channel (NTE—white; Aβ—blue; CD31—red) are displayed in B-D. Scale bar indicates 50 μm

concentration of the ligand. PET detects all radioactivity, including radioactivity originating from the blood volume of the brain and unbound radioligand in the brain parenchyma. Hence, to detect differences in the antibodies' intrabrain binding to Aβ deposits, PET has to be conducted when blood radioactivity is low and when unbound radioligand has been eliminated from the brain, motivating the choice to do PET imaging at 144 hours post-injection.

PET and ex vivo measurements of radioactivity revealed that brain concentrations of unmodified Bapi in tg-ArcSwe mice were higher than expected and almost the same as for Bapi-TXB2. The reason for the relatively high Bapi signal in PET could be partly explained by the slower elimination of [^{124}I]Bapi from blood, and thus, a higher background signal from blood and unbound radioligand in this group. This was confirmed by the images, as the Bapi signal from the tissue around the brain was higher than what was observed for Bapi-TXB2. Images, when normalized for blood concentrations therefore gave a better picture of the concentration equilibrium across the BBB. We speculate that the fairly high brain retention of Bapi originates from antibody interactions with cerebral amyloid angiopathy (CAA) and/or potentially

"leakage" into the brain parenchyma at these sites, leading to a further increase in radioactivity signal detected by PET in tg-ArcSwe mice. Similar results have been reported for the murine version of Bapi, 3D6, appearing as "hot spots" in ex vivo autoradiography of old [^{125}I]3D6-injected tg-ArcSwe mice.[27] To investigate whether this effect would be less prominent in younger mice, [^{125}I]Bapi, and [^{125}I]Bapi-TXB2 were injected in 12-month-old tg-ArcSwe mice, expected to have less CAA. Ex vivo autoradiography images indicated that [^{125}I]Bapi accumulated in high concentration "hot spots," with minor distribution to other parts of the brain, a phenomenon that was even more prominent in 18 months old mice. Also [^{125}I]Bapi-TXB2 accumulated to some extent in hot spots, but in addition, displayed a uniform distribution pattern throughout the parenchyma. The highest retention was observed in areas of abundant Aβ deposition, especially cortex, hippocampus, and thalamus, and also to some extent in the cerebellum, where pathology starts to emerge at this age.[23,30] This pattern resembles what we have previously reported for brain penetrating Aβ antibodies[30] and represents successful transcytosis of [^{125}I]Bapi-TXB2 across the BBB of brain capillaries. This was confirmed by nuclear track emulsion autoradiography in combination with immunostaining of Aβ and the vascular marker CD31, demonstrating that [^{125}I]Bapi-TXB2 crossed the BBB to interact with parenchymal Aβ pathology, while [^{125}I]Bapi did not, and that hot spots of Bapi were found around vessels with adjacent Aβ pathology. Moreover, although hot spots were present in young mice, Bapi-TXB2 showed almost 6-fold higher brain-to-blood ratio compared with Bapi in these mice, which is markedly higher than in old mice (Table 2), and probably more truly reflects the brain penetrating capacity of Bapi-TXB2. The reduced transcytosis efficiency of TXB2 when attached to Bapi (compared with fusion to an Fc fragment) in combination with the assumed binding to CAA thus decreased the difference in brain retention between Bapi and Bapi-TXB2. Further studies will be needed to determine whether TXB2 could more efficiently transfer a different Aβ antibody, with less CAA binding, into the brain.

We believe a threefold increased brain uptake for Bapi, or any other intrabrain acting Aβ antibody, is very relevant from a therapeutic perspective. Clinical studies have shown that the amount of administered therapeutic anti-Aβ antibodies *aducanumab*[31] is positively correlated with their beneficial effects; a high dose results in more efficient clearance of brain Aβ and a slower decline in cognition compared to a low dose. However, the risk of side effects such as amyloid-related imaging abnormalities (ARIA) caused by microhemorraghes of the BBB and edema is increased with the higher dose; 13% of the patients in a 3 mg/kg aducanumab dose group and 47% in a 10 mg/kg of aducanumab dose group experienced ARIA. Side effects, including ARIA, are most likely related to systemic concentrations. Hence, reduction of the systemically administered dose with maintained brain concentrations could be a very important step toward a safe use of immunotherapy for AD.

In conclusion, this study demonstrates that the high affinity TXB2 TfR1 binder can be used to shuttle large protein cargo such as an IgG into the brain. The effectiveness of the TXB2-VNAR may be dependent on its cargo. Development of novel brain shuttles is likely to be of great importance for immunotherapy of neurodegenerative diseases such as AD.

ACKNOWLEDGMENTS

We are grateful to Lars NG Nilsson, who developed and characterized the mouse model, and to Jos Buijs for assistance with analysis of Ligand Tracer experiments. The molecular imaging work in this study was performed at the SciLifeLab Pilot Facility for Preclinical PET-MRI, a Swedish nationally available imaging platform at Uppsala University, Sweden, financed by the Knut and Alice Wallenberg Foundation. This work was supported by grants from the Swedish research council (2012-1593, 2017-02413, and 2018-02715), Alzheimerfonden, Åhlénstiftelsen, Torsten Söderbergs stiftelse, Hjärnfonden, Hedlunds stiftelse, Åke Wibergs stiftelse, Magnus Bergwalls stiftelse, Stohnes stiftelse, Stiftelsen för gamla tjänarinnor and Goljes stiftelse.

CONFLICT OF INTEREST

PS, FSW, and JLR are paid employees of Ossianix Inc Ossianix Inc has filed patents on the subject matter of this manuscript.

AUTHOR CONTRIBUTIONS

D. Sehlin, S. Syvänen, P. Stocki, and G. Hultqvist designed the study; P. Stocki designed and expressed the antibodies; D. Sehlin, S. Syvänen, and T. Gustavsson performed all experiments; D. Sehlin and S. Syvänen wrote the manuscript with input from all authors. All authors contributed to interpretation of results.

REFERENCES

1. Lannfelt L, Relkin NR, Siemers ER. Amyloid-ss-directed immunotherapy for Alzheimer's disease. *J Intern Med*. 2014;275:284-295.
2. Bard F, Cannon C, Barbour R, et al. Peripherally administered antibodies against amyloid beta-peptide enter the central nervous system and reduce pathology in a mouse model of Alzheimer disease. *Nat Med*. 2000;6:916-919.
3. Pardridge WM. CSF, blood-brain barrier, and brain drug delivery. *Expert Opin Drug Deliv*. 2016;13:963-975.
4. Pardridge WM. Re-engineering therapeutic antibodies for Alzheimer's disease as blood-brain barrier penetrating bi-specific antibodies. *Expert Opin Biol Ther*. 2016;16:1455-1468.
5. Clark AJ, Davis ME. Increased brain uptake of targeted nanoparticles by adding an acid-cleavable linkage between transferrin and the nanoparticle core. *Proc Natl Acad Sci U S A*. 2015;112:12486-12491.

6. Johnsen KB, Burkhart A, Melander F, et al. Targeting transferrin receptors at the blood-brain barrier improves the uptake of immunoliposomes and subsequent cargo transport into the brain parenchyma. *Sci Rep*. 2017;7:10396.
7. Wyatt EA, Davis ME. Method of establishing breast cancer brain metastases affects brain uptake and efficacy of targeted, therapeutic nanoparticles. *Bioeng Transl Med*. 2019;4:30-37.
8. Niewoehner J, Bohrmann B, Collin L, et al. Increased brain penetration and potency of a therapeutic antibody using a monovalent molecular shuttle. *Neuron*. 2014;81:49-60.
9. Hultqvist G, Syvanen S, Fang XT, Lannfelt L, Sehlin D. Bivalent brain shuttle increases antibody uptake by monovalent binding to the transferrin receptor. *Theranostics*. 2017;7:308-318.
10. Yu YJ, Zhang Y, Kenrick M, et al. Boosting brain uptake of a therapeutic antibody by reducing its affinity for a transcytosis target. *Sci Transl Med*. 2011;3:84ra44.
11. Syvanen S, Hultqvist G, Gustavsson T, et al. Efficient clearance of Abeta protofibrils in AbetaPP-transgenic mice treated with a brain-penetrating bifunctional antibody. *Alzheimer's Res Ther*. 2018;10:49.
12. Couch JA, Yu YJ, Zhang Y, et al. Addressing safety liabilities of TfR bispecific antibodies that cross the blood-brain barrier. *Sci Transl Med*. 2013;5:183ra57.
13. Zuchero YJ, Chen X, Bien-Ly N, et al. Discovery of novel blood-brain barrier targets to enhance brain uptake of therapeutic antibodies. *Neuron*. 2016;89:70-82.
14. Muruganandam A, Tanha J, Narang S, Stanimirovic D. Selection of phage-displayed llama single-domain antibodies that transmigrate across human blood-brain barrier endothelium. *FASEB J*. 2002;16:240-242.
15. Webster CI, Caram-Salas N, Haqqani AS, et al. Brain penetration, target engagement, and disposition of the blood-brain barrier-crossing bispecific antibody antagonist of metabotropic glutamate receptor type 1. *FASEB J*. 2016;30:1927-1940.
16. Stocki P, Szary JM, Rasmussen CLM, et al. Blood-brain barrier transport using a highaffinity, brain-selective VNAR (Variable Domain of New Antigen Receptor) antibody targeting transferrin receptor 1. *bioRxiv*, 816900. https://doi.org/10.1101/816900
17. Salloway S, Sperling R, Gilman S, et al. A phase 2 multiple ascending dose trial of bapineuzumab in mild to moderate Alzheimer disease. *Neurology*. 2009;73:2061-2070.
18. Lo M, Kim HS, Tong RK, et al. Effector-attenuating substitutions that maintain antibody stability and reduce toxicity in mice. *J Biol Chem*. 2017;292:3900-3908.
19. Lord A, Kalimo H, Eckman C, Zhang XQ, Lannfelt L, Nilsson LN. The Arctic Alzheimer mutation facilitates early intraneuronal Abeta aggregation and senile plaque formation in transgenic mice. *Neurobiol Aging*. 2006;27:67-77.
20. Lord A, Englund H, Soderberg L, et al. Amyloid-beta protofibril levels correlate with spatial learning in Arctic Alzheimer's disease transgenic mice. *FEBS J*. 2009;276:995-1006.
21. Philipson O, Hammarstrom P, Nilsson KP, et al. A highly insoluble state of Abeta similar to that of Alzheimer's disease brain is found in Arctic APP transgenic mice. *Neurobiol Aging*. 2009;30:1393-1405.
22. Sehlin D, Fang XT, Cato L, Antoni G, Lannfelt L, Syvanen S. Antibody-based PET imaging of amyloid beta in mouse models of Alzheimer's disease. *Nat Commun*. 2016;7:10759.
23. Sehlin D, Fang XT, Meier SR, Jansson M, Syvanen S. Pharmacokinetics, biodistribution and brain retention of a bispecific antibody-based PET radioligand for imaging of amyloid-beta. *Sci Rep*. 2017;7:17254.
24. Wang E, Bjorkelund H, Mihaylova D, et al. Automated functional characterization of radiolabeled antibodies: a time-resolved approach. *Nucl Med Commun*. 2014;35:767-776.
25. Loening AM, Gambhir SS. AMIDE: a free software tool for multimodality medical image analysis. *Mol Imaging*. 2003;2:131-137.
26. Ma Y, Hof PR, Grant SC, et al. A three-dimensional digital atlas database of the adult C57BL/6J mouse brain by magnetic resonance microscopy. *Neuroscience*. 2005;135:1203-1215.
27. Gustafsson S, Gustavsson T, Roshanbin S, et al. Blood-brain barrier integrity in a mouse model of Alzheimer's disease with or without acute 3D6 immunotherapy. *Neuropharmacology*. 2018;143:1-9.
28. Sehlin D, Syvanen S, Faculty M. Engineered antibodies: new possibilities for brain PET? *Eur J Nucl Med Mol Imaging*. 2019;46:2848-2858.
29. Fang XT, Hultqvist G, Meier SR, Antoni G, Sehlin D, Syvanen S. High detection sensitivity with antibody-based PET radioligand for amyloid beta in brain. *NeuroImage*. 2019;184:881-888.
30. Meier SR, Syvanen S, Hultqvist G, et al. Antibody-based in vivo PET imaging detects amyloid-beta reduction in Alzheimer transgenic mice after BACE-1 inhibition. *J Nucl Med*. 2018;59:1885-1891.
31. Sevigny J, Chiao P, Bussiere T, et al. The antibody aducanumab reduces Abeta plaques in Alzheimer's disease. *Nature*. 2016;537:50-56.

SUPPORTING INFORMATION

Additional Supporting Information may be found online in the Supporting Information section.

How to cite this article: Sehlin D, Stocki P, Gustavsson T, et al. Brain delivery of biologics using a cross-species reactive transferrin receptor 1 VNAR shuttle. *The FASEB Journal*. 2020;34:13272–13283. https://doi.org/10.1096/fj.202000610RR